Age of Information-Aware Crowd-Finding for Emergency Search: A Game-Theoretic Analysis with Heterogeneous Costs

Antonio Tangaro
Department of Information Engineering
University of Padova, Italy
antonio.tangaro@studenti.unipd.it

***Abstract*—When a child goes missing in a crowded area, every second counts. Modern crowd-finding networks like Apple's Find My leverage millions of volunteer devices to detect beacons from missing persons, yet participation is voluntary and costly. This paper investigates this tension through the lens of game theory, using Age of Information (AoI) to capture the time-critical nature of emergency search. The analysis reveals that selfish behavior leads to systematic under-participation: volunteers consider only their private benefit while ignoring the positive externality they create for others. Closed-form expressions are derived showing that the participation gap scales as $\Delta k \approx \ln(N)/\rho$, where N is the number of volunteers and ρ the coverage probability. Monte Carlo simulations validate the detection probability formula with less than 1% error, while agent-based simulations demonstrate up to 53 percentage points efficiency loss in rescue success rate (Table III). The model is further extended to heterogeneous costs, where each volunteer has a private participation cost drawn from a distribution, deriving threshold equilibria and incentive mechanisms. A Stackelberg analysis shows that platform subsidies can implement the social optimum in the homogeneous case and achieve socially optimal participation in expectation under heterogeneous costs, providing actionable guidance for emergency response system design.**

***Index Terms*—Age of Information, game theory, mobile crowdsensing, emergency search, Nash equilibrium, heterogeneous costs, Stackelberg game.**

I. Introduction

Imagine a scenario where an elderly person with dementia wanders away from their care facility. Their family activates a tracking beacon, and within minutes, thousands of nearby smartphones begin scanning for the signal. This is not science fiction; it describes the operating principle of crowd-sourced localization networks like Apple's Find My, which leverages over a billion devices worldwide to locate missing persons and objects [1]. Similar scenarios have been studied in the mobile crowdsensing literature, including the "Finding Nemo" system designed specifically for locating lost children in crowds [2].

The effectiveness of such systems hinges on voluntary participation. Each volunteer who enables beacon scanning incurs real costs: battery drain, bandwidth consumption, privacy exposure, and cognitive effort. Meanwhile, the benefits of successful detection (a rescued child, a found pet, a recovered valuable) are shared by all. This creates a classic public goods problem where rational individuals may contribute less than what society collectively needs.

In emergency scenarios, the *freshness* of location information becomes paramount. A detection report from five minutes ago may lead rescuers to a location the target has already left. Age of Information (AoI) [3], [4] provides the natural metric for this setting, measuring the time elapsed since the last successful update. Lower AoI means fresher information and higher probability of successful rescue.

While prior work has studied AoI optimization and strategic behavior in crowdsensing separately (see Section II), the specific combination of AoI-aware metrics with strategic analysis of emergency crowd-finding as a public good remains unexplored.

This paper presents a comprehensive game-theoretic analysis of volunteer participation in emergency crowd-finding networks. The system is modeled as a non-cooperative game where volunteers balance AoI-derived benefits against participation costs. Closed-form expressions are derived for Nash equilibrium and social optimum, and it is proven that selfish behavior leads to systematic under-participation. The analysis is then extended to heterogeneous costs, a more realistic model where volunteers have different opportunity costs. Stackelberg incentive mechanisms are designed that can implement the social optimum. Monte Carlo and agent-based simulations validate the theoretical predictions and demonstrate the practical impact of under-participation on rescue success rates.

The remainder of this paper is organized as follows. Section II positions this work within related literature on crowd-finding, AoI, and strategic crowdsensing. Section III presents the system model including the physical environment, detection model, and utility functions. Section IV develops the game-theoretic analysis for homogeneous costs. Section V extends the model to heterogeneous costs. Section VI provides numerical validation and experimental results. Section VII concludes with implications and future directions.

II. Related Work

Crowd-finding and object localization systems. Crowd-sourced localization networks leverage ubiquitous mobile devices to detect beacons from missing persons or objects. Empirical and security/privacy analyses of large-scale systems (e.g., Find My) highlight feasibility and system-level risks [1]. Complementary protocols address privacy-preserving object finding via cryptographic mechanisms [5]. Emergency-oriented designs such as "Finding Nemo" demonstrate technical viability for locating lost children in crowds [2]. However, this line largely assumes willing participation and does not model strategic under-participation when scanning is privately costly.

Information freshness and Age of Information (AoI). Traditional metrics such as delay or throughput do not directly capture information staleness. AoI formalizes timeliness as time since the last successful update [3], and surveys consolidate its theoretical foundations and design trade-offs [4], including the "update-or-wait" principle [6]. AoI has also been incorporated into sensing and control settings, including AoI-driven task/pricing formulations [7] and learning-based AoI minimization in UAV crowdsensing [8]. These works motivate AoI as the appropriate metric for time-critical search, but typically assume cooperative sources or centrally controlled update behavior.

Incentives and strategic behavior in mobile crowdsensing. A substantial literature studies incentives when participants act strategically. Surveys provide taxonomies of mechanisms (e.g., auctions, Stackelberg games, reputation) and highlight the platform cost vs. quality trade-off [9], [10], while systems perspectives discuss architectural constraints and practical deployment challenges [11]. Socially-aware hierarchical incentives further model complex interaction structures [12], [13]. Nevertheless, much of this line focuses on data acquisition where reward can be tied to contributor-specific value, whereas emergency crowd-finding exhibits a strong public-good externality: detection benefits are shared and non-excludable.

Game-theoretic AoI and AoI-aware incentives. Recent work combines AoI with game theory, showing that strategic behavior can degrade freshness [14] and extending to participatory/federated ecosystems [15]. Efficiency loss under selfish users has been characterized via Price of Anarchy in related learning/crowd settings [16]. Stackelberg mechanisms have been proposed for AoI-aware crowdsensing and vehicular timeliness constraints [17], [18]. Unlike data markets where providers compete for contributor-specific payoffs, emergency crowd-finding differs because the benefit is primarily social and shared.

Summary. A common implicit assumption across most related strands is that either (i) participants cooperate to generate updates, or (ii) incentives can be modeled as a data market with contributor-specific value. In contrast, we study emergency crowd-finding as an AoI-driven public-goods participation game. To the best of our knowledge, this combination has not been analyzed in closed form. We (i) derive closed-form Nash equilibrium and socially optimal participation, quantifying systematic under-participation; (ii) extend to heterogeneous private costs via threshold Bayesian equilibria; and (iii) design Stackelberg subsidies that implement the social optimum in the homogeneous model and implement the socially optimal participation level in expectation under heterogeneous costs.

III. System Model

This section presents an emergency crowd-finding scenario where volunteers with mobile devices assist in locating a missing target within a bounded search area. The target emits periodic beacon signals that can be detected by nearby devices and reported to a central control center.

A. Physical Environment

The search area is modeled as a square region $\mathcal{A} = [0, L]^2 \subset \mathbb{R}^2$ with side length $L > 0$. A single target located at position $\mathbf{x}_T \in \mathcal{A}$ emits periodic beacon signals. The target position is modeled as uniformly distributed over $\mathcal{A}$, reflecting uncertainty about their location.

The system comprises N volunteers, indexed by the set $\mathcal{N} = \{1, \ldots, N\}$, each carrying a mobile device capable of detecting beacons. Volunteer i occupies position $\mathbf{x}_i$ drawn independently and uniformly from $\mathcal{A}$. A central control center aggregates location updates from volunteers and coordinates rescue efforts.

B. Detection Model

A volunteer successfully detects the target beacon if the Euclidean distance falls within detection radius $R > 0$:

$$d_i = \|\mathbf{x}_i - \mathbf{x}_T\|_2 \leq R \tag{1}$$

For uniformly distributed positions and ignoring boundary effects when $R \ll L$, each volunteer covers the target with probability $\rho = \pi R^2 / L^2$, termed the coverage ratio. More importantly, Eq. (2) is a mean-field coverage model relying on spatial independence; clustering or correlated mobility would modify the effective coverage and is discussed as a limitation in Section VII.

Each volunteer makes a binary participation decision $a_i \in \{0, 1\}$, where $a_i = 1$ indicates active scanning and $a_i = 0$ indicates inactivity. The total number of active volunteers is $k = \sum_{i=1}^{N} a_i$.

Lemma 1 (Coverage Probability). *Given k active volunteers with independent uniformly distributed positions, the probability that at least one covers the target is:*

$$P_{\text{det}}(k) = 1 - (1 - \rho)^k \tag{2}$$

The proof follows from independence: each volunteer fails to cover the target with probability $(1 - \rho)$, so all k fail with probability $(1 - \rho)^k$. This detection probability is strictly increasing and concave in k, exhibiting diminishing returns to additional participation.

C. Age of Information

The Age of Information at the control center measures the time elapsed since the last successful location update. In discrete time with slots $t \in \{0, 1, 2, \ldots\}$, the AoI evolves as:

$$\Delta(t+1) = \begin{cases} 0 & \text{if detection occurs during slot } t \\ \Delta(t) + 1 & \text{otherwise} \end{cases} \tag{3}$$

That is, at the end of slot t, if a detection occurred during that slot, then $\Delta(t+1) = 0$; otherwise $\Delta(t+1) = \Delta(t) + 1$.

Under stationary conditions with detection probability $P_{\text{det}}(k)$ per slot, the time between successful updates follows a geometric distribution. Following the analysis in [14], the expected time-average AoI is:

$$\bar{\Delta}(k) = \frac{1}{P_{\text{det}}(k)} - 1 = \frac{(1-\rho)^k}{1-(1-\rho)^k} \tag{4}$$

Eq. (4) holds under a discrete-time Bernoulli detection model with per-slot success probability $P_{\text{det}}(k)$ and i.i.d. detection outcomes across slots (e.g., i.i.d. spatial snapshots or sufficiently mixing mobility). In Section VI-G we relax i.i.d. via correlated mobility and use Eq. (4) as a baseline mean-field predictor.

This expression captures the intuition that more active volunteers yield fresher information: as k increases, $P_{\text{det}}(k)$ approaches 1 and $\bar{\Delta}(k)$ approaches 0.

D. Utility Functions

Volunteer participation is modeled as a static game of complete information $\mathcal{G} = \langle \mathcal{N}, \{A_i\}, \{U_i\} \rangle$. The benefit from fresh information is captured by:

$$f(\bar{\Delta}) = \frac{B}{1+\bar{\Delta}} \tag{5}$$

where $B > 0$ is the maximum benefit when $\bar{\Delta} = 0$. Substituting the expected AoI from (4) yields:

$$f(\bar{\Delta}(k)) = B \cdot P_{\text{det}}(k) \tag{6}$$

Each active volunteer incurs cost $c > 0$ representing battery consumption, privacy concerns, and effort. The utility of volunteer i given action profile $\mathbf{a}$ is:

$$U_i(\mathbf{a}) = B \cdot P_{\text{det}}(k) - c \cdot a_i \tag{7}$$

This utility structure embodies the public goods nature of the problem: all volunteers receive benefit $B \cdot P_{\text{det}}(k)$ regardless of their participation, but only active volunteers pay the cost c. This creates incentives for free-riding that drive the under-participation result.

The baseline model assumes homogeneous volunteers with identical costs c, complete information about parameters (N, ρ, B, c), independent positions and decisions, and rational utility maximization. Section V relaxes the homogeneity assumption.

IV. Game-Theoretic Analysis

This section characterizes the Nash equilibrium, social optimum, and efficiency loss for the homogeneous cost model.

A. Nash Equilibrium

Given the symmetry of identical players, the analysis focuses on symmetric Nash equilibria. The marginal increase in detection probability from one additional volunteer is $P_{\text{det}}(k+1) - P_{\text{det}}(k) = \rho(1-\rho)^k$, which decreases exponentially in k.

A volunteer considers participation worthwhile when the marginal benefit exceeds the cost. When k_{-i} others are active, volunteer i's marginal utility from participating is:

$$\Delta U_i(k_{-i}) = B\rho(1-\rho)^{k_{-i}} - c \tag{8}$$

Theorem 1 (Nash Equilibrium). *A symmetric configuration with k^* active volunteers is a Nash equilibrium if and only if $B\rho(1-\rho)^{k^*} \leq c \leq B\rho(1-\rho)^{k^*-1}$. The equilibrium participation level is:*

$$k^* = \left\lfloor 1 + \frac{\ln(c/B\rho)}{\ln(1-\rho)} \right\rfloor \tag{9}$$

when $c \leq B\rho$, and $k^* = 0$ otherwise.

The proof verifies that active volunteers prefer participation over defection, and inactive volunteers prefer free-riding over joining. The equilibrium condition requires the marginal benefit to bracket the cost from above and below.

B. Social Optimum

The social welfare aggregates utilities across all volunteers:

$$W(k) = N \cdot B \cdot P_{\text{det}}(k) - k \cdot c \tag{10}$$

The key difference from individual decision-making is that social welfare accounts for the benefit to all N volunteers, not just the participant. Adding the k-th volunteer is socially beneficial when $NB\rho(1-\rho)^{k-1} \geq c$.

Theorem 2 (Social Optimum). *The socially optimal participation level is:*

$$k^{opt} = \left\lfloor 1 + \frac{\ln(c/NB\rho)}{\ln(1-\rho)} \right\rfloor \tag{11}$$

when $c \leq NB\rho$, and $k^{opt} = 0$ otherwise.

Since at most N volunteers exist, we implicitly apply the saturation $k \leftarrow \min\{N, \max\{0, k\}\}$ to the closed-form expressions (9) and (11). This does not affect the subsequent analysis in the considered parameter ranges.

C. Under-Participation Gap

Comparing the equilibrium conditions reveals systematic under-participation. At Nash equilibrium, a volunteer participates when their private marginal benefit $B\rho(1-\rho)^{k-1}$ exceeds c. At the social optimum, participation continues until the social marginal benefit $NB\rho(1-\rho)^{k-1}$ falls below c. Since $N \geq 1$, the social threshold is satisfied for strictly more volunteers.

Theorem 3 (Participation Gap). *The gap between social optimum and Nash equilibrium scales as:*

$$\Delta k = k^{opt} - k^* \approx \frac{\ln N}{\rho} \tag{12}$$

for small coverage ratio ρ.

This result has important implications: the under-participation problem worsens with more volunteers (larger N) and sparser coverage (smaller ρ). Eq. (12) is an asymptotic scaling for $\rho \ll 1$. In any finite system, participation is bounded by $0 \leq k^*, k^{\text{opt}} \leq N$, hence $\Delta k \leq N$. Therefore, when $\ln(N)/\rho \gg N$, Eq. (12) should be interpreted as predicting near-maximal under-participation: Nash participation can drop close to 0 while the social optimum remains close to N. For example, with $N = 100$ and $\rho \approx 0.01$, $\ln(N)/\rho \approx 460 \gg N$, indicating that the gap can approach its upper bound N in the critical cost regime. This phenomenon is consistent with the Price of Anarchy analysis in related AoI games [16].

D. Price of Anarchy

The Price of Anarchy quantifies efficiency loss:

$$\text{PoA} = \frac{W(k^{\text{opt}})}{W(k^*)} \tag{13}$$

We evaluate (13) on parameter regions where $W(k^*) > 0$; when $W(k^*) = 0$, we adopt the convention PoA $= +\infty$.

The PoA increases as cost approaches the critical threshold $c \to B\rho$, where Nash participation collapses to zero while the social optimum remains positive. In this regime, the denominator approaches zero while the numerator remains bounded, causing the PoA to diverge. This identifies a "danger zone" where platform intervention is most critical.

E. Stackelberg Incentive Mechanism

A platform can improve outcomes by offering incentive payments, as proposed in various crowdsensing contexts [12], [17], [19]. The interaction is modeled as a Stackelberg game where the platform (leader) announces payment $p \geq 0$ per active volunteer, and volunteers (followers) respond with modified utility $U_i^p = B \cdot P_{\text{det}}(k) - (c-p) \cdot a_i$. We seek the minimum subsidy that implements the social optimum.

Theorem 4 (Minimum Implementing Subsidy)**.** *To implement social optimum k^{opt}, the platform offers:*

$$p^* = \max\left\{0,\ c - B\rho(1-\rho)^{k^{opt}-1}\right\} \tag{14}$$

with total budget $p^* \cdot k^{opt}$. If $p^* = 0$, no subsidy is needed.

The subsidy bridges the gap between private and social marginal benefit. When the gap is large, the required payment approaches the full cost c, making incentive provision expensive but necessary for achieving efficient outcomes.

V. Extension to Heterogeneous Costs

The homogeneous model provides clean analytical results but assumes all volunteers have identical costs, an unrealistic simplification. In practice, volunteers differ in battery capacity, privacy sensitivity, and opportunity costs. This section extends the analysis to heterogeneous costs.

A. Heterogeneous Cost Model

Each volunteer i has a private participation cost c_i drawn independently from a continuous distribution F supported on $[c_{\min}, c_{\max}]$ with $0 < c_{\min} < c_{\max}$. The cost c_i is known only to volunteer i, creating a game of incomplete information. We study a symmetric Bayesian Nash equilibrium where F and system parameters are common knowledge, while each c_i is privately observed by player i.

The analysis focuses on the uniform distribution $F(c) = (c - c_{\min})/(c_{\max} - c_{\min})$ for analytical tractability, though the framework extends to other log-concave distributions. The mean cost is $\bar{c} = (c_{\min} + c_{\max})/2$, and the heterogeneity ratio $c_{\max}/c_{\min}$ measures cost dispersion.

B. Threshold Equilibrium

With heterogeneous costs, equilibrium takes a threshold form: volunteer i participates if and only if $c_i \leq \bar{c}(k^*)$, where $\bar{c}(k)$ is the cost threshold when k volunteers participate.

Theorem 5 (Threshold Equilibrium – Mean-Field)**.** *Under a mean-field approximation where an individual's action does not affect the aggregate k, the Nash equilibrium is characterized by threshold $\bar{c}^* = B\rho(1-\rho)^{k^*}$ and participation level k^* satisfying:*

$$k^* = N \cdot F(\bar{c}^*) \tag{15}$$

The mean-field approximation evaluates the marginal benefit at k rather than $k-1$, which is accurate for large N. For $N = 100$, this approximation is validated numerically in Table II.

This fixed-point equation admits a unique solution in our tested regimes. Volunteers with cost below the threshold find participation worthwhile given the equilibrium detection probability; those above prefer free-riding.

The equilibrium can be computed via iteration: starting from an initial guess, compute the threshold $\bar{c}(k) = B\rho(1-\rho)^k$, update $k \leftarrow N \cdot F(\bar{c}(k))$, and repeat until convergence. In all tested parameter regimes, this iteration converged reliably with appropriate damping.

C. Social Optimum with Order Statistics

The social planner selects which volunteers should participate to maximize welfare. With heterogeneous costs, optimal selection follows a greedy rule: activate volunteers in order of increasing cost until marginal benefit falls below marginal cost.

Theorem 6 (Heterogeneous Social Optimum)**.** *The socially optimal participation level k^{opt} is the largest integer k such that:*

$$NB\rho(1-\rho)^{k-1} \geq \mathbb{E}[c_{(k)}] \tag{16}$$

where $c_{(k)}$ denotes the k-th order statistic (the k-th lowest cost among N volunteers).

For the uniform distribution, the expected k-th order statistic is $\mathbb{E}[c_{(k)}] = c_{\min} + (c_{\max} - c_{\min}) \cdot k/(N+1)$. This allows closed-form computation of the social optimum.

D. Comparison: Homogeneous vs Heterogeneous

How does heterogeneity affect equilibrium outcomes? With heterogeneous costs, low-cost volunteers consistently participate even when mean cost is high, providing a stable base of coverage. This contrasts with the homogeneous model where participation is all-or-nothing at the individual level.

The numerical experiments in Section VI reveal that heterogeneity reduces the participation gap compared to a homogeneous model with the same mean cost. The intuition is that the social planner can selectively recruit low-cost volunteers, while in the homogeneous model, all-or-nothing participation creates sharper cliffs in the welfare function.

E. Incentive Design for Heterogeneous Costs

The Stackelberg mechanism extends naturally. With incentive $p \geq 0$, the threshold becomes $\bar{c}^*(p) = B\rho(1-\rho)^{k^*(p)} + p$, shifting the participation threshold upward. We seek the minimum subsidy that implements the socially optimal participation level.

Theorem 7 (Minimum Implementing Subsidy)**.** *To implement the socially optimal participation level in expectation, the platform offers:*

$$p^* = \max\left\{0,\ \bar{c}^{opt} - B\rho(1-\rho)^{k^{opt}}\right\} \tag{17}$$

where $\bar{c}^{opt} = F^{-1}(k^{opt}/N)$ is the cost of the marginal volunteer at the optimum. If $p^* = 0$, no subsidy is needed as the Nash equilibrium already achieves the social optimum.

Because costs are random, the realized number of participants is random under any uniform payment. The proposed p^* sets the marginal type at quantile k^{opt}/N indifferent, so that $\mathbb{E}[k] = k^{\text{opt}}$ (and $k/N \to F(\bar{c})$ as $N \to \infty$ by the law of large numbers).

The total incentive budget is $p^* \cdot k^{\text{opt}}$, which exceeds the homogeneous case because the platform must compensate higher-cost volunteers who would not participate voluntarily.

VI. Numerical Results

This section validates the theoretical predictions through Monte Carlo simulation and demonstrates practical impact through agent-based modeling.

A. Experimental Setup

The baseline configuration uses search area $L = 500$m, $N = 100$ volunteers, detection radius $R = 30$m, and benefit $B = 10$. This yields coverage ratio $\rho = \pi R^2/L^2 \approx 0.0113$ and critical cost threshold $B\rho \approx 0.113$.

For heterogeneous experiments, a uniform cost distribution with spread ratio $c_{\max}/c_{\min} = 2.0$ is used, varying mean cost across the informative range $[0.1B\rho, 0.95B\rho]$.

TABLE I: Validation of $P_{\text{det}}(k) = 1 - (1-\rho)^k$

k	Theory	Simulated	Error (%)
5	0.0553	0.0555 $\pm$ 0.0006	0.4
20	0.2035	0.2016 $\pm$ 0.0009	0.9
50	0.4337	0.4328 $\pm$ 0.0011	0.2
100	0.6794	0.6775 $\pm$ 0.0012	0.3

B. Detection Probability Validation

The detection probability formula is first validated using static Monte Carlo simulation with i.i.d. volunteer positions. For each value of k, 100 runs of 2000 time steps each are sampled, computing the empirical detection rate. Values are reported as mean $\pm$ standard deviation across runs.

Table I shows excellent agreement between theory and simulation across all tested configurations, with relative error consistently below 1%. This validates the analytical model under ideal conditions.

C. Homogeneous Cost Sweep

Figure 1 shows Nash equilibrium and social optimum participation as cost varies across the informative range. Nash participation k^* decreases sharply as cost increases, while social optimum k^{opt} remains at $N = 100$ throughout. We intentionally sweep c around the private critical threshold $B\rho$ to isolate the under-participation regime; in this range $c \ll NB\rho$, so the social optimum saturates at N. The shaded region represents the participation gap, quantifying the efficiency loss from selfish behavior.

At low costs ($c < 0.3B\rho$), the gap is small and both outcomes achieve near-perfect coverage. As cost increases toward the critical threshold, Nash participation collapses while social optimum remains high, creating severe efficiency loss. At $c = 0.95B\rho$, Nash achieves only $k^* = 5$ active volunteers versus $k^{\text{opt}} = 100$ at the social optimum.

D. Heterogeneous Cost Analysis

The effect of heterogeneity on equilibrium outcomes is examined next. Figure 2 shows the effect of varying the spread ratio $c_{\max}/c_{\min}$ while holding mean cost fixed.

As heterogeneity increases, Nash participation k^* decreases slightly because the threshold equilibrium becomes more sensitive to the cost distribution shape. However, the participation gap relative to social optimum also changes: heterogeneity can either increase or decrease efficiency depending on the cost regime.

The key insight is that heterogeneity provides robustness. In the homogeneous model, all volunteers have the same participation threshold, creating knife-edge behavior. With heterogeneous costs, low-cost volunteers provide a stable participation floor even when mean cost is high.

Figure 3 directly compares homogeneous and heterogeneous models across a cost sweep with the same mean cost. The heterogeneous model exhibits smoother participation curves and smaller efficiency losses in the critical cost regime.

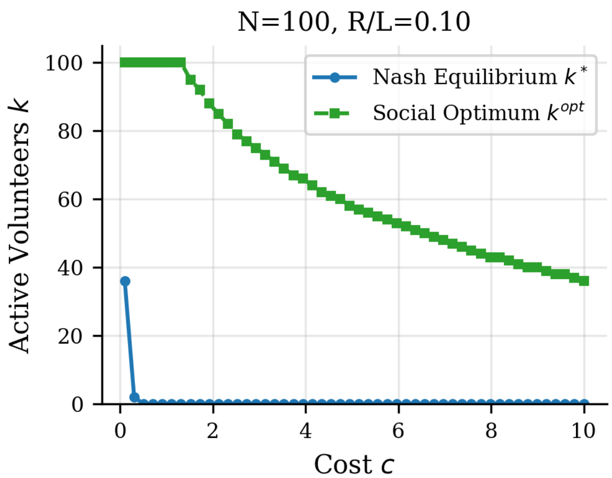

Fig. 1: Participation vs. normalized cost $c/(B\rho)$. Nash equilibrium (blue) collapses as cost approaches the critical threshold, while social optimum (green) remains at full participation. Parameters: see Section VI-A.

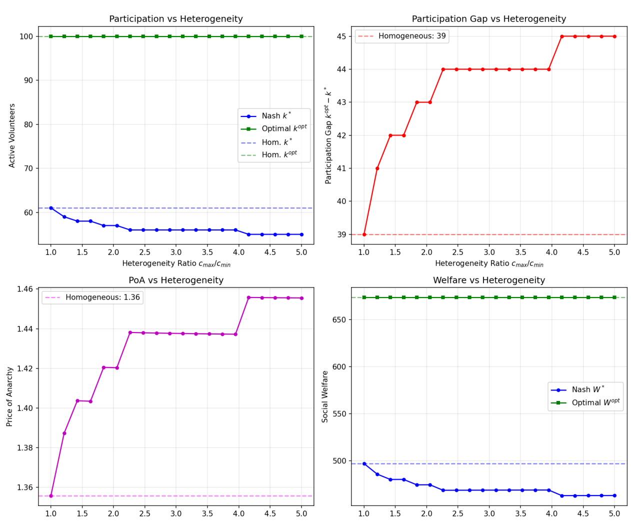

Fig. 2: Effect of heterogeneity ratio $c_{\max}/c_{\min}$ on equilibrium. Top left: participation levels. Top right: participation gap. Bottom left: Price of Anarchy. Bottom right: social welfare. Parameters: see Section VI-A.

E. Stackelberg Incentive Comparison

Figure 4 compares subsidies across homogeneous and heterogeneous settings. The heterogeneous model requires higher per-volunteer payments because the platform must compensate marginal volunteers with costs above the Nash threshold.

The welfare improvement from subsidies is substantial in both cases. Defining improvement as $(W^{\text{opt}} - W^{\text{NE}})/W^{\text{NE}}$, the efficiency gain from moving from Nash to social optimum exceeds 200% in the homogeneous model and 100% in the heterogeneous model at high costs.

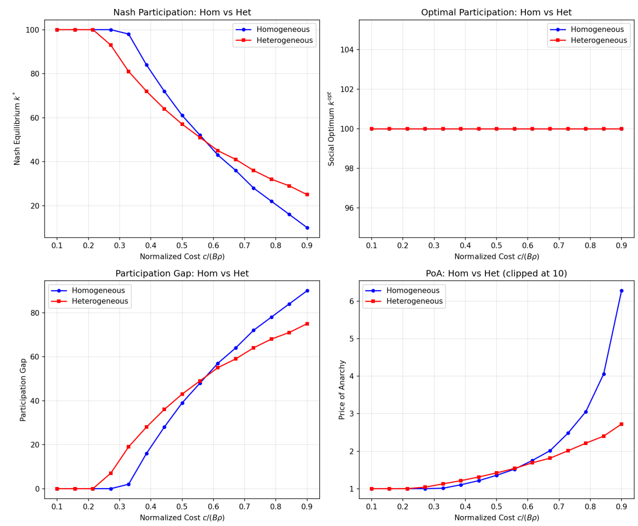

Fig. 3: Comparison of homogeneous (blue) and heterogeneous (red) models. Top row: Nash and optimal participation. Bottom row: participation gap and Price of Anarchy. Parameters: see Section VI-A.

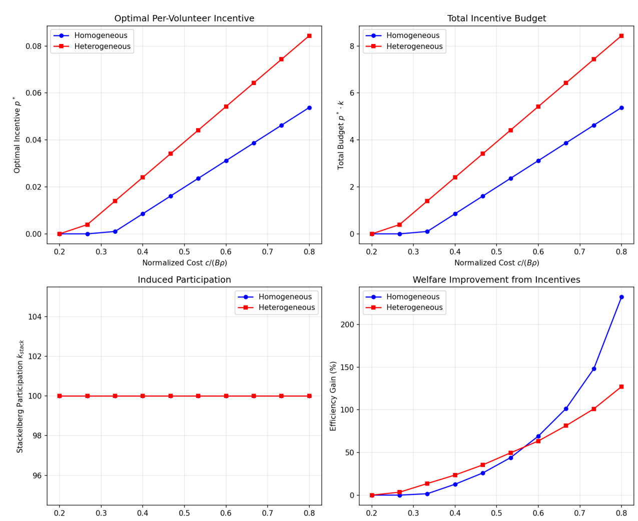

Fig. 4: Stackelberg subsidy comparison. Top row: subsidy p^* and total budget. Bottom row: induced participation and welfare improvement. Parameters: see Section VI-A.

F. Monte Carlo Validation of Heterogeneous Model

Table II validates the heterogeneous equilibrium predictions against Monte Carlo simulation. For each spread ratio, 200 cost realizations are sampled, the analytical prediction is computed, and comparison is made against simulated equilibrium behavior.

The analytical predictions match simulation with less than 1% error across all tested configurations, validating the threshold equilibrium characterization.

TABLE II: Heterogeneous Model Validation (200 MC runs)

Spread	k^* (Ana.)	k^* (Sim.)	Error (%)
1.5	58	58.47	0.80
2.0	57	57.31	0.54
3.0	56	55.95	0.10
4.0	55	55.25	0.45

TABLE III: Dynamic Simulation: Rescue Success Rate

$c/(B\rho)$	k^*	k^{opt}	Nash (%)	Optimal (%)
0.10	100	100	100	100
0.50	64	100	100	100
0.72	30	100	93	100
0.87	12	100	73	100
0.95	5	100	47	100

G. Dynamic Simulation: Rescue Success

To demonstrate practical impact beyond theoretical validation, an agent-based simulation is developed where volunteers move toward random waypoints and the target performs a bounded random walk. This setting introduces temporal correlation and violates the i.i.d. assumption, but shows that the under-participation phenomenon persists qualitatively.

Rescue success requires maintaining AoI below 30 steps during a 60-step response period. Table III shows rescue success rates across the cost sweep. At high costs, Nash equilibrium achieves only 47% success versus 100% at the social optimum. This 53 percentage point efficiency loss has direct implications for emergency response outcomes.

VII. Conclusions

This paper presented a comprehensive game-theoretic analysis of volunteer participation in emergency crowd-finding networks, using Age of Information to capture the time-critical nature of rescue operations.

The main findings are as follows. First, selfish behavior leads to systematic under-participation, with the gap scaling as $\ln(N)/\rho$. This creates severe efficiency loss in the critical cost regime where Nash participation collapses while social optimum remains high. Second, the heterogeneous cost extension reveals that cost dispersion provides robustness: low-cost volunteers maintain a stable participation floor even when mean cost is high, reducing efficiency loss compared to the knife-edge behavior of homogeneous models. Third, Stackelberg incentive mechanisms can implement the social optimum in the homogeneous model and achieve socially optimal participation in expectation under heterogeneous costs, though the required budget increases with cost heterogeneity. Fourth, Monte Carlo validation confirms the analytical predictions with sub-1% error, while agent-based simulation demonstrates up to 53 percentage points efficiency loss in rescue success rate under realistic conditions.

These results have practical implications for emergency response system design. Platform operators should implement incentive mechanisms (whether monetary subsidies, gamification, or reputation systems) to bridge the gap between individual rationality and social welfare. The heterogeneous cost analysis suggests that targeted incentives for marginal volunteers may be more cost-effective than uniform subsidies.

Several limitations merit future investigation. The model assumes complete information about network parameters; extending to Bayesian games where volunteers have uncertain beliefs would increase realism. The single-shot participation decision could be generalized to repeated interactions with learning dynamics. Multiple concurrent targets would introduce competition among searches. Finally, spatial clustering changes the mapping $k \mapsto P_{\text{det}}(k)$ by breaking the independence assumption; the analysis can be re-run by replacing Eq. (2) with an empirically calibrated $P_{\text{det}}(\cdot)$ from mobility traces.

Despite these limitations, this analysis provides the first rigorous game-theoretic foundation for understanding strategic participation in emergency crowd-finding, offering both theoretical insight and actionable guidance for system designers seeking to optimize life-saving outcomes.

Acknowledgment

This work was completed as part of the Game Theory course at the University of Padova under the supervision of Prof. Leonardo Badia.

References

[1] A. Heinrich, M. Hollick, T. Schneider, M. Stute, and C. Weinert, "Who can find my devices? Security and privacy of Apple's crowd-sourced Bluetooth location tracking system," in *Proc. Privacy Enhancing Technologies Symposium (PETS)*, 2021, pp. 227–245.

[2] K. Liu and X. Li, "Finding Nemo: Finding your lost child in crowds via mobile crowd sensing," in *Proc. IEEE MASS*, 2014, pp. 1–9.

[3] S. Kaul, R. Yates, and M. Gruteser, "Real-time status: How often should one update?" in *Proc. IEEE INFOCOM*, 2012, pp. 2731–2735.

[4] R. D. Yates, Y. Sun, D. R. Brown, S. K. Kaul, E. Modiano, and S. Ulukus, "Age of information: An introduction and survey," *IEEE Journal on Selected Areas in Communications*, vol. 39, no. 5, pp. 1183–1210, May 2021.

[5] J. Sun, R. Zhang, X. Jin, and Y. Zhang, "SecureFind: Secure and privacy-preserving object finding via mobile crowdsourcing," *IEEE Transactions on Wireless Communications*, vol. 15, no. 3, pp. 1716–1728, Mar. 2016.

[6] Y. Sun, E. Uysal-Biyikoglu, R. D. Yates, C. E. Koksal, and N. B. Shroff, "Update or wait: How to keep your data fresh," *IEEE Transactions on Information Theory*, vol. 63, no. 11, pp. 7492–7508, Nov. 2017.

[7] H. Gao, H. Xu, C. Zhou, H. Zhai, P. Ni, and Z. Han, "Dynamic task pricing in mobile crowdsensing: An age-of-information-based queueing game scheme," *IEEE Internet of Things Journal*, vol. 9, no. 21, pp. 21 278–21 291, 2022.

[8] Z. Dai, C. H. Liu, Y. Ye, R. Han, Y. Yuan, G. Wang, and J. Tang, "AoI-minimal UAV crowdsensing by model-based graph convolutional reinforcement learning," in *Proc. IEEE INFOCOM*, 2022, pp. 1029–1038.

[9] V. S. Dasari, B. Kantarci, M. Pouryazdan, L. Foschini, and M. Girolami, "Game theory in mobile crowdsensing: A comprehensive survey," *Sensors*, vol. 20, no. 7, p. 2055, 2020.

[10] X. Zhang, Z. Yang, W. Sun, Y. Liu, S. Tang, K. Xing, and X. Mao, "Incentives for mobile crowd sensing: A survey," *IEEE Communications Surveys and Tutorials*, vol. 18, no. 1, pp. 54–67, 2016.

[11] A. Capponi, C. Fiandrino, B. Kantarci, L. Foschini, D. Kliazovich, and P. Bouvry, "A survey on mobile crowdsensing systems: Challenges, solutions, and opportunities," *IEEE Communications Surveys and Tutorials*, vol. 21, no. 3, pp. 2419–2465, 2019.

[12] J. Nie, J. Luo, Z. Xiong, D. Niyato, and P. Wang, "A Stackelberg game approach toward socially-aware incentive mechanisms for mobile crowdsensing," *IEEE Transactions on Wireless Communications*, vol. 18, no. 1, pp. 724–738, Jan. 2019.

[13] J. Nie, J. Luo, Z. Xiong, D. Niyato, P. Wang, and H. V. Poor, “A multi-leader multi-follower game-based analysis for incentive mechanisms in socially-aware mobile crowdsensing,” *IEEE Transactions on Wireless Communications*, vol. 20, no. 3, pp. 1457–1471, Mar. 2021.

[14] L. Badia, “Age of information from two strategic sources analyzed via game theory,” in *Proc. IEEE CAMAD*, 2021, pp. 1–6.

[15] A. Buratto, A. Mora, A. Bujari, and L. Badia, “Game theoretic analysis of AoI efficiency for participatory and federated data ecosystems,” in *Proc. IEEE ICC Workshops*, 2023, pp. 1301–1306.

[16] B. Li and J. Liu, “Achieving information freshness with selfish and rational users in mobile crowd-learning,” *IEEE Journal on Selected Areas in Communications*, vol. 39, no. 5, pp. 1266–1276, May 2021.

[17] M. Xiao, Y. Xu, J. Zhou, J. Wu, S. Zhang, and J. Zheng, “AoI-aware incentive mechanism for mobile crowdsensing using Stackelberg game,” in *Proc. IEEE INFOCOM*, 2023, pp. 1–10.

[18] X. Chen, L. Zhang, Y. Pang, B. Lin, and Y. Fang, “Timeliness-aware incentive mechanism for vehicular crowdsourcing in smart cities,” *IEEE Transactions on Mobile Computing*, vol. 21, no. 9, pp. 3373–3387, Sep. 2022.

[19] Y. Xu, M. Xiao, J. Wu, S. Zhang, and G. Gao, “Incentive mechanism for spatial crowdsourcing with unknown social-aware workers: A three-stage Stackelberg game approach,” *IEEE Transactions on Mobile Computing*, vol. 22, no. 8, pp. 4698–4713, Aug. 2023.